JOURNAL OF GUIDANCE, CONTROL, AND DYNAMICS
Vol. 32, No. 5, September–October 2009

Optimal Control of a Librating Electrodynamic Tether Performing a Multirevolution Orbit Change

Robert E. Stevens*
U.S. Naval Academy, Annapolis, Maryland 21402
and
William P. Baker†
Air Force Institute of Technology, Wright–Patterson Air Force Base, Ohio 45433

DOI: 10.2514/1.42679

Satellites that use low-thrust propulsion systems for maneuvering, although efficient, can take a long time to complete significant orbit changes. Determining the nonlinear optimal controls for such multirevolution maneuvers using the instantaneous orbital state dynamics can be riddled with numerical errors and are often subject to long computation times, due to the large number of discretization nodes required by the optimization algorithm. An approach to optimal control of an electrodynamic tether is examined using averaged orbital state dynamics as constraints instead of instantaneous dynamic constraints. A mean-square libration state is introduced in the dynamic model that captures the average of the out-of-plane libration of the tether. A sample long-term optimal orbit change maneuver of a librating electrodynamic tether subject to atmospheric drag is investigated. The method of averaging is employed to transform the optimal control problem from the time domain into Fourier space, in which the complex problem is significantly reduced to a Zermelo-type problem that is solved using a pseudospectral method. To validate the dynamic model of averaged states, the instantaneous states are propagated from the initial conditions using the resulting optimal controls.

Nomenclature

A = effective cross-sectional area of the tether system
a = average semimajor axis
$\mathbf{B}$ = local Earth magnetic flux density vector
B_i^* = ballistic coefficient for the ith body
$\mathbf{D}$ = resultant atmospheric drag force
e = average eccentricity
ε = ratio of maximum Lorenz torque to gravity gradient torque, scaling parameter
$\mathbf{F}$ = resultant Lorenz force on the electrodynamic tether
g = path constraint
I = control current
I_m = maximum allowable root-mean-square current
i = average inclination
L = tether length
m = system mass
$\tilde{m}$ = effective reduced mass
n = orbital mean motion
r = radial distance with respect to Earth's center
$\mathbf{u}$ = control vector of Fourier coefficients
v = orbital velocity
$\mathbf{x}$ = system state vector of averaged orbital elements and mean-square libration
z = mean-square out-of-plane libration state
γ = flight-path angle
γ_m = Earth magnetic dipole moment
ϕ = out-of-plane libration angle
μ = Earth's gravitational parameter
ν = true anomaly
ρ = atmospheric density
$\hat{\boldsymbol{\rho}}$ = tether orientation vector
ω = average argument of perigee

Received 22 December 2008; revision received 14 May 2009; accepted for publication 15 May 2009.

*Assistant Professor, Department of Aeronautics and Astronautics; resteven@aol.com.
†Associate Professor, Department of Mathematics and Statistics; william.baker@afit.edu.

I. Introduction

SATELLITES that use electrodynamic tethers (EDTs) for orbital maneuvering have great advantages over propellant-based systems because the Earth's ionosphere and magnetic field provide the necessary ingredients for propulsion. By running a current through a long straight wire in a magnetic field, a Lorenz force is generated, which propels the wire in a direction perpendicular to both the local magnetic field vector and the current in the wire. The Earth itself provides the magnetic field, and the ionosphere serves as both a ready source of electrons and also completes the circuit necessary for the flow of current in the EDT wire. A good overview of the concept along with the associated challenges and history is provided in [1]. The two-ball EDT model used in this paper is depicted in Fig. 1. The force magnitude depends on the current, length of wire, and the wire orientation with respect to the local magnetic field. A longer tether yields a greater thrusting force; however, it comes at the expense of greater drag at lower altitudes. Additionally, a tether will tend to librate about the center of mass as the gravity gradient torque competes with the torques induced by both atmospheric drag and the Lorenz force. An uncontrolled EDT with a constant direct current running through it will eventually go unstable, as demonstrated by Pelaez et al. [2]. However, by controlling the Lorenz force via the current in the wire through variable resistance, the satellite system could maneuver to new orbits while maintaining stable libration without propellant, albeit at a slower rate than chemical maneuvering rockets or kick motors. Because of the slow orbital changes afforded by the low thrust available, an orbit transfer requires a long time to reach a desired orbit; thus, a method of control is needed to achieve optimal trajectories that span many orbital revolutions.

Determining optimal controls for satellites that maneuver over the course of many orbital revolutions can be challenging and computationally intensive when states and controls are considered on short time scales of a few orbital revolutions. Williams [3] demonstrated a method of determining EDT optimal control using instantaneous nonlinear perturbation equations of motion and libration as dynamic constraints and solved an optimal control

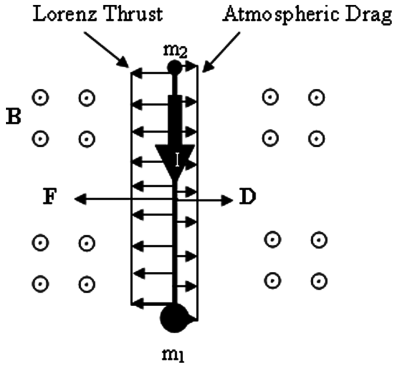

Fig. 1 Electrodynamic tether force model.

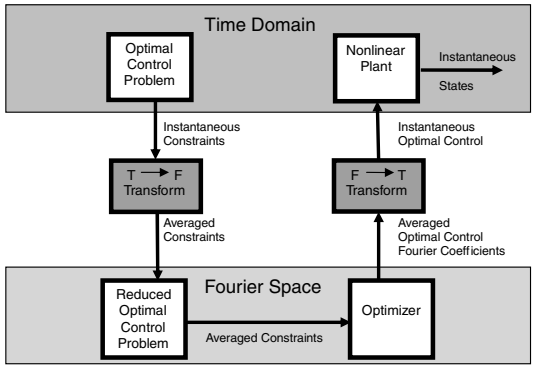

Fig. 2 Optimal control in Fourier space.

problem by direct transcription using nonlinear programming software. This method is shown to be effective in determining controls that execute a small short-term orbit maneuver using an electrodynamic tether for thrust with a dynamic model that includes libration. However, the solver required hundreds of collocation node points to capture all the small state variations that occur in a single day of maneuvering. The enormous number of discretization nodes required to determine optimal controls for a larger orbit transfer spanning months would be extremely susceptible to round-off errors and long computation times. In many low-thrust maneuvering situations, the instantaneous orbit state will vary only slightly from an average state, which tends to change only slowly, taking long periods of time (i.e., many orbital revolutions) to change significantly. Carroll [4] introduced a way to express long-term EDT behavior for given control strategies that were further explored by Tragesser and San [5], who applied the method of averaging to demonstrate nonoptimal control of the average states. This method has the advantage of avoiding the computational burden associated with controlling the rapidly changing instantaneous states, thereby enabling the determination of control strategies for larger orbit transfers spanning longer time periods. The results, however, are not optimal and libration is not considered. A method combining the advantages of both approaches is presented in [6] in which the constraints of a given optimal control problem are transformed into a Fourier space by modeling the averaged orbital state dynamics instead of the instantaneous dynamics. It was assumed, however, that the tether was nadir-pointing and nonlibrating, but in reality, we would need to account for the librations of the long tether, both to manage stability and to establish a higher-fidelity dynamic model. The subject of this paper is to expand the model introduced in [6] to include libration dynamics for large-time-scale maneuvers by applying the method of averaging to optimal control theory. The diagram in Fig. 2 shows how some complex periodic optimal control problems (OCPs) may be significantly reduced to Zermelo-type[‡] problems [7] using the method of averaging to transform constraints into a Fourier space. This transformation eliminates all dependence on variables that change rapidly with time (i.e., vary within a single revolution), and the resulting averaged states and controls will only depend on variables that change slowly over many revolutions. It should be noted that because this method controls a system's time-averaged states, the resulting optimal trajectory must cover many revolutions for averaging to be effective. For multirevolution optimal control problems that cannot take advantage of averaging, a more general method such as the approach introduced by Ross et al. [8] may be more suitable if round-off errors due to iterative propagation steps are considered insignificant. The method presented here, however, contains no propagation steps and uses very few collocation node points for optimization and is thus less susceptible to numerical round-off errors and solves the OCP in a single step without iteration. The remainder of this paper will describe the construction and solution of an EDT optimal control problem in a Fourier space using the method of averaging and a dynamic model that includes libration.

[‡]In 1923, German mathematician Ernst Zermelo posed the problem of navigating a boat from point A to point B in minimum time, factoring in wind and current. The solution is not a straight-line path.

II. Dynamic Model

The dynamic model is addressed in two parts: one part that describes the average orbital motion and one that describes the libration motion. The objective is to achieve a model that is independent of the rapidly varying effects that occur only over short time intervals and captures only the slow, secular behavior of the system over a long time. With such a model, we can impose a dynamic constraint in a general OCP form such that the averaged states are constrained or controlled throughout the maneuver, yielding an optimal trajectory to a desired end state.

A. Orbital Motion

The Lorenz force generated along a wire channeling an electric current is given by

$$\mathbf{F} = I\mathbf{L} \times \mathbf{B}$$

where I represents tether current (the control), $\mathbf{B}$ represents the Earth's local magnetic flux density vector, and $\mathbf{L}$ is the tether length vector pointing in the direction from the upper end mass m_2 to the lower end mass m_1. The tether geometry and current direction that yield a positive transverse thrust are shown in Fig. 1. The control current is assumed to be periodic, because periodic control is the only control that will yield secular changes in the averaged states. This control is a function of slowly changing Fourier control coefficients (varying only on a large time scale T) expressed using a basis of relevant harmonics of a Fourier series:

$$I = I[\mathbf{u}(T), \nu] = I_m \mathbf{\Psi}^T(\nu)\mathbf{u}(T)$$

where I_m represents the maximum allowable rms current, and the controller is defined using the relevant harmonics of the Fourier series. The controller consists of Fourier coefficients and a basis set, which is defined using the dc component and first two harmonics of a Fourier series for the discussion in this paper:

$$\mathbf{u}\,(T) = [u_1, u_2, u_3, u_4, u_5]^T$$

$$\mathbf{\Psi}(\nu) = [1, \cos\nu, \sin\nu, \cos 2\nu, \sin 2\nu]^T$$

Had the model included effects and perturbations that change with respect to multiple time scales, additional control terms and basis sets could have been included to capture additional frequencies [9], but this set is sufficient for the model chosen here. The local magnetic flux density for an Earth-orbiting satellite is modeled as

$$\mathbf{B} = \frac{\gamma_m}{r^3}\begin{bmatrix} -2\sin(\omega+\nu)\sin i \\ \cos(\omega+\nu)\sin i \\ \cos i \end{bmatrix} = \begin{bmatrix} B_r \\ B_t \\ B_n \end{bmatrix}$$

where γ_m represents the Earth's magnetic dipole moment; i is the inclination relative to the magnetic equator; and B_r, B_t, and B_n represent the magnetic flux density vector components in the radial, transverse, and orbit normal directions, respectively (i.e., $\hat{e}_r$, $\hat{e}_t$, and $\hat{e}_n$ directions in Fig. 3). For a near-circular orbit, the drag force on the entire tether system is given by

$$\mathbf{D} = -\frac{1}{2}B^*\rho(r)\frac{\mu}{r}\hat{\mathbf{e}}_\mathbf{t}$$

where $\rho(r)$ represents the average air density at radial distance r, and B^* is the average ballistic coefficient of the entire tether. Here, the ballistic coefficient is defined as

$$B^* = \frac{C_d A}{m} \tag{1}$$

where C_d is the average coefficient of drag, A is the average cross-sectional area perpendicular to the velocity vector, and m is the system mass. The averaged orbital state dynamics of the EDT to order e^2 are derived in [6] and are repeated here for convenience:

$$\begin{aligned}
\frac{da}{dt} &\approx 2Ca\cos i(u_1 + u_2 e) - 2D \\
\frac{dh}{dt} &\approx C\cos i\left[\left(\frac{3h}{2}\right)u_1 + \left(\frac{h}{e}\right)u_2 + \left(\frac{k}{e}\right)u_3 + \left(\frac{h}{4} + \frac{hk^2}{2e^2}\right)u_4 \right. \\
&\quad \left. + \left(\frac{k}{4} + \frac{(k^2-h^2)k}{4e^2}\right)u_5\right] - \frac{D}{a}\left(1 + \frac{a}{h^*}\right)h \\
\frac{dk}{dt} &\approx C\cos i\left[\left(\frac{3k}{2}\right)u_1 + \left(\frac{k}{e}\right)u_2 - \left(\frac{h}{e}\right)u_3 + \left(\frac{k}{4} - \frac{h^2 k}{2e^2}\right)u_4 \right. \\
&\quad \left. + \left(-\frac{h}{4} + \frac{(h^2-k^2)h}{4e^2}\right)u_5\right] - \frac{D}{a}\left(1 + \frac{a}{h^*}\right)k \\
\frac{di}{dt} &\approx -C\sin i\left[\left(\frac{1}{2}\right)u_1 + \left(\frac{k^2-h^2}{4e^2}\right)u_4 - \left(\frac{hk}{2e^2}\right)u_5\right]
\end{aligned} \tag{2}$$

where $C = L\gamma_m/nma^4$ represents the thrust per unit current and the drag rate is $D = B^*\mu\rho(a)/2na$. The states used here are averaged orbital parameters, not instantaneous, expressed using a partial equinoctial set, where $h = e\sin\omega$ and $k = e\cos\omega$ to avoid singularity when considering circular orbits. The dynamics of these average states do not contain a fast time variable such as ν; thus, the average states only vary slowly over long time scales. These equations assume a nonlibrating nadir-pointing tether, and so to achieve accurate controls and maintain libration stability, we need to include libration dynamics into the model.

B. Libration

The instantaneous libration dynamic equations of motion are derived in the Appendix and may be written for the in-plane and out-of-plane librations, respectively, as

$$\ddot{\theta} = -\ddot{\nu} + 2(\dot{\theta} + \dot{\nu})\dot{\phi}\tan\phi - 3\frac{\mu}{r^3}\sin\theta\cos\theta + \frac{Q_\theta}{\tilde{m}L^2\cos^2\phi} \tag{3}$$

$$\ddot{\phi} = -\left[(\dot{\theta} + \dot{\nu})^2 + 3\frac{\mu}{r^3}\cos^2\theta\right]\sin\phi\cos\phi + \frac{Q_\phi}{\tilde{m}L^2} \tag{4}$$

where ν is the true anomaly, $\tilde{m}$ is the effective reduced mass of the system that accounts for the mass distribution, and θ and ϕ are the in- and out-of-plane libration angles, respectively. Dots indicate differentiation with respect to clock time t [i.e., $(\dot{}) = d(\,)/dt$]. The scalars Q_θ and Q_ϕ are the generalized forces affecting the in- and out-of-plane libration angles, respectively, due to a combination of electrodynamic Lorenz and aerodynamic drag forces. It has been shown that an unperturbed inert (unpowered) tether in a circular orbit librates in and out of the orbital plane about an equilibrium point with marginal stability (see [10], for example). An uncontrolled EDT with constant dc running through it, however, will go unstable over time [2]. We desire to establish a periodic controller that will enable an optimal orbital transfer while simultaneously driving libration amplitude to a desired end state within specified bounds. Unfortunately, straightforward averaging of the derivative of the libration angle as we did with the orbital state derivative would yield zero for a tether librating about nadir. Control cannot be achieved for a state that is always zero, and so a different approach is required to capture the librational motion in a Fourier space.

To simplify the problem, in-plane libration is ignored and we will focus on controlling the out-of-plane libration depicted in Fig. 3. In-plane libration is not resonant with the periodic controller or the orbital motion, because it evolves with frequency $\omega_\theta = \sqrt{3}n$, where n is the mean motion of the satellite, and thus it does not grow very quickly. The out-of-plane libration has frequency $\omega_\phi = 2n$, which is commensurate with the frequency of the orbital motion and the controller, resulting in more rapid growth (or decay) over time. With this justification for ignoring the in-plane libration in mind, we derive a new state that captures only the out-of-plane libration (hereafter simply called *libration*, unless otherwise stated).

A constraint in Fourier space must not contain any functions of a fast time variable (i.e., trigonometric functions of ν). Averaging serves to eliminate dependence on this fast time variable, leaving only variables changing slowly with time in the equations of motion. To accomplish this, a new state is devised: the mean-square value of a tether's out-of-plane libration. Whether power is applied to the tether or not, the libration mean square is proportional to the maximum angle reached throughout the pendular cycle. For an unpowered (inert) librating EDT, the mean-square value is exactly half of the square of the libration magnitude ϕ_m (i.e., $\phi^2_{\text{rms}} = \phi^2_m/2$). This relationship is approximate for a powered EDT as long as the perturbation due to the electromagnetic torque is relatively small. Deriving an expression that describes the librational mean-square behavior provides a way to understand the behavior of the magnitude of the librational motion over a long time. Thus, constraining the mean-square trajectory for a given orbital maneuver is tantamount to bounding the envelope that contains the librational motion of the tether over long time durations.

Unfortunately, the librational equations of motion given in Eqs. (3) and (4) have no closed-form solution that will enable us to capture the libration amplitude changes over long time scales. The good news, however, is that assuming small libration angles, we may linearize the equations of motion, thus decoupling the in- and out-of-plane libration equations of motion. To start, we will ignore the aerodynamic torque and only consider the electrodynamic torque in the libration controller model and write

$$\begin{aligned}
\ddot{\phi} + 4\phi &= \frac{Q_{\phi e}}{\tilde{m}L^2} \\
&= \frac{(m_2 - m_1)\gamma_m}{2m\tilde{m}\mu} I_m \sin i(\tilde{k}(T)\cos\nu - \tilde{h}(T)\sin\nu)\Psi^T(\nu)\mathbf{u}(T) \\
&= \varepsilon\sin i(\tilde{k}\cos\nu - \tilde{h}\sin\nu) \\
&\quad \times (u_1 + u_2\cos\nu + u_3\sin\nu + u_4\cos 2\nu + u_5\sin 2\nu)
\end{aligned} \tag{5}$$

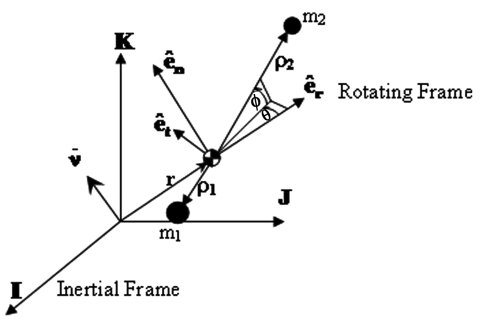

Fig. 3 Rotating frame coordinates.

where the independent variable has been changed to ν so that $(\dot{}) = d(\,)/d\nu$. This equation is expressed using a partial equinoctial element set described in the previous section, where $\tilde{k} = k/e$ and $\tilde{h} = h/e$. Both $\tilde{k}$ and $\tilde{h}$ are order-1 quantities that are themselves averages that vary slowly over a long time. Adopting the convention established in [2,11], the nondimensional small parameter ε is defined as the ratio of the maximum electrodynamic torque to the gravity gradient torque and corresponds to the powered part of expansion:

$$\varepsilon = \frac{\text{max electrodynamic torque}}{\text{gravity gradient torque}} = I_m \frac{(m_2 - m_1)\gamma_m}{2m\tilde{m}\mu} \tag{6}$$

For a uniform 1.5 A rms, 500 kg tether system in low Earth orbit, with an upper end mass of 230 kg and a lower end mass of 220 kg, this parameter is about 0.0026. The slow-time-scale variable T is a scaled version of the clock time t and the true anomaly, related by the scaling parameter ε such that

$$T = \varepsilon t = \varepsilon \frac{\nu}{n} \tag{7}$$

We have chosen the nondimensional scale factor here to be the torque ratio defined in Eq. (6) for reasons that will soon be apparent. Only small changes to the known periodic libration motion of the inert tether over short time spans will occur as long as the electrodynamic torque is small compared with the gravity gradient (i.e., $\varepsilon \ll 1$). In transforming the controls from the short-time-scale domain to Fourier space, we exchange a single control variable (current as a function of a fast time variable) for five control variables (the five Fourier coefficients in $\mathbf{u}(T)$ that are functions of a slow time variable).[§] Expanding the right-hand side term in the differential equation in Eq. (5) and through liberal use of trigonometric identities, we determine an exact solution to the linearized equation:

$$\begin{aligned}\phi(\nu, T) &= \phi_o(\nu, T) + \varepsilon\phi_1(\nu, \mathbf{u}(T)) \\ &= \phi_m(T)\cos 2(\nu - \nu_o) + \varepsilon \sin i(\tilde{k}K - \tilde{h}H)\end{aligned} \tag{8}$$

where

$$\begin{aligned}K(\nu, \mathbf{u}(T)) &= \frac{u_2}{8} + \frac{1}{3}\left(u_1 + \frac{u_4}{2}\right)\cos\nu + \frac{u_5}{6}\sin\nu - \frac{u_3}{8}\nu\cos 2\nu \\ &\quad + \frac{u_2}{8}\nu\sin 2\nu - \frac{u_4}{10}\cos 3\nu - \frac{u_5}{10}\sin 3\nu \\ H(\nu, \mathbf{u}(T)) &= \frac{u_3}{8} + \frac{u_5}{6}\cos\nu - \frac{1}{3}\left(\frac{u_4}{2} - u_1\right)\sin\nu - \frac{u_2}{8}\nu\cos 2\nu \\ &\quad + \frac{u_3}{8}\nu\sin 2\nu + \frac{u_5}{10}\cos 3\nu - \frac{u_4}{10}\sin 3\nu\end{aligned}$$

and $\phi_m(T)$ is the initial amplitude of the librational motion, which is considered constant over a single orbital period, but changes slowly over time.

One restriction due to the linearization is that the second term on the right-hand side of Eq. (8) must be less than order 1 (i.e., $\varepsilon\nu \ll 1$). Therefore, to ensure the accuracy of the solution, the duration is limited to $\nu \ll 1/\varepsilon$ (note the explicit ν terms present in K and H). This is a reasonable assumption when we consider a small electrodynamic torque due to nearly equal end masses and a uniform current in the tether. For a scaled maximum electrodynamic torque of $\varepsilon = 0.0026$, this maximum allowable duration corresponds to about 60 orbital revolutions. Eventually, a long-duration optimal control problem will be discretized into smaller intervals that are much shorter than this limit so that this approximate solution is valid for each subinterval. Linking the subintervals together, the long-term maneuver will consist of states and Fourier coefficient controls that are constant within each subinterval, but vary slowly over the course of the whole trajectory. The first term on the right side of Eq. (8) represents the homogeneous solution, indicating that a tether without any electrodynamic torque would continually librate at twice the orbital frequency. Perturbations come through the small electrodynamic torque of order ε imparted on the tether over a long time. Whether these perturbations destabilize or stabilize the libration depends on the slowly changing control terms contained in K and H. A thorough derivation of periodic libration-angle solutions is provided in [11] for an EDT with a steady dc current.

For an unpowered tether, or one in which the center of mass is collocated with the center of force on the tether (thus, no Lorenz torque, and so $\varepsilon\mathbf{u}(T) = \mathbf{0}$), or an equatorial orbit in which $i = 0$, the solution to Eq. (8) is the homogeneous solution:

$$\phi_o(\nu, T) = \phi_m(T)\cos(2(\nu - \nu_0))$$

Presuming that the periodic control may be started at any time during the libration cycle, we assume the peak of a libration cycle corresponds with $\nu_0 = 0$, then

$$\phi_o(\nu, T) = \phi_m(T)\cos 2\nu$$

Using this model, the libration is controlled through the remaining $\mathcal{O}(\varepsilon)$ term in Eq. (8). Now we define the libration mean-square state as

$$z(\nu, T) = \phi^2_{\text{rms}} \equiv \frac{1}{2\pi}\int_{\nu}^{\nu+2\pi} \phi^2(\xi, T)\mathrm{d}\xi \tag{9}$$

This state is always positive and is itself an average over a period by definition. Furthermore, for short time intervals, such as a few orbital periods, the libration amplitude change is negligible and the relationship between the state z and the amplitude may be expressed as

$$2z = 2\phi^2_{\text{rms}} \approx \phi^2_m$$

Substituting Eq. (8) into Eq. (9), we write

$$\begin{aligned}z(\nu, T) &= \frac{1}{2\pi}\int_{\nu}^{\nu+2\pi} \phi^2(\xi, T)\mathrm{d}\xi \\ &= \frac{1}{2\pi}\int_{\nu}^{\nu+2\pi} [\phi_o(\xi, T) + \varepsilon\phi_1(\xi, \mathbf{u}(T))]^2\mathrm{d}\xi \\ &= \frac{1}{2\pi}\int_{\nu}^{\nu+2\pi} \phi_o^2 + 2\varepsilon\phi_o\phi_1 + \varepsilon^2\phi_1^2\mathrm{d}\xi\end{aligned} \tag{10}$$

Because $\phi_o(\nu, T)$ and $\phi_1(\nu, \mathbf{u}(T))$ are both considered 2π-periodic in ν over a single period, the whole integrand in Eq. (10) is assumed to be 2π-periodic. This assumption is valid because $\mathbf{u}(T)$ and $\phi_m(T)$ do not change significantly over the short 2π interval; therefore, the limits of the definite integral may be considered from 0 to 2π without the loss of generality. Thus, the secular change in z due to the Lorenz torque averaged over one period is

$$\begin{aligned}z(T) &= \frac{1}{2\pi}\int_0^{2\pi} \phi_o^2 + 2\varepsilon\phi_o\phi_1 + \varepsilon^2\phi_1^2\mathrm{d}\nu \\ &= \frac{1}{2\pi}\int_0^{2\pi} \phi_o^2 + 2\phi_m\varepsilon\sin i\cos 2\nu(\tilde{k}K - \tilde{h}H) \\ &\quad + \varepsilon^2\sin^2 i(\tilde{k}K - \tilde{h}H)^2\mathrm{d}\nu\end{aligned}$$

Because the next step in the derivation will be to integrate, terms that will average to zero after integration may be omitted, which yields

$$\begin{aligned}z(T) &= \frac{1}{2\pi}\int_0^{2\pi} \phi_o^2\mathrm{d}\nu + \frac{\phi_m \sin i}{4}\frac{1}{2\pi}\int_0^{2\pi} \varepsilon\nu\cos 2\nu[(\tilde{h}u_2 - \tilde{k}u_3)\cos 2\nu \\ &\quad + (\tilde{k}u_2 - \tilde{h}u_3)\sin 2\nu]\mathrm{d}\nu \\ &\quad + \frac{\sin^2 i}{64}\frac{1}{2\pi}\int_0^{2\pi} \varepsilon^2\nu^2[\tilde{k}(u_3\cos 2\nu + u_2\sin 2\nu) \\ &\quad + \tilde{h}(u_2\cos 2\nu - u_3\sin 2\nu)]^2\mathrm{d}\nu + \mathcal{O}(\varepsilon^2\nu)\end{aligned} \tag{11}$$

[§]We refer to the variable as a *slow* time variable, because variables dependent on change slowly over long time scales. By contrast, the variables ν and t are considered as *fast* time variables, because variables dependent on these cycle on a short time scale (e.g., a single revolution).

The first integral term in Eq. (11) is the inert tether libration mean-square value. Secular changes enter the system through the remaining terms that have an explicit dependence on ν. Over a single period, the change in z is very small, due to the scaling factor ε. Recalling Eq. (7), we substitute the slow time variable T for $\varepsilon\nu$, consider it constant over the limits of the definite integral, and remove it from the integrand. This slow time variable affects the secular growth (or decay) of the z state only over large spans of time, and so only the sinusoidal functions of ν are averaged through integration. Physically, the mean-squared value of libration changes approximately linearly with T to first order over short time intervals. The plot in Fig. 4 depicts the nearly linear small change in the z state over one period. Substituting the slow time variable into Eq. (11) and expanding yields

$$z(T) = \frac{1}{2\pi}\int_0^{2\pi} \phi_o^2 \mathrm{d}\nu + \frac{nT}{4}\phi_m \sin i \frac{1}{2\pi}\int_0^{2\pi}\Big[(\tilde{h}u_2 - \tilde{k}u_3)\cos^2 2\nu + (\tilde{k}u_2 - \tilde{h}u_3)\frac{1}{2}\sin 4\nu\Big]\mathrm{d}\nu + \frac{n^2T^2\sin^2 i}{64}\frac{1}{2\pi}\int_0^{2\pi}[\tilde{k}^2(u_3^2\cos^2 2\nu + u_2^2\sin^2 2\nu) + \tilde{h}^2(u_2^2\cos^2 2\nu + u_3^2\sin^2 2\nu) - 2\tilde{h}\,\tilde{k}\,u_2u_3]\mathrm{d}\nu + \mathcal{O}(\varepsilon T) \tag{12}$$

Finally, we perform the integration with respect to true anomaly and take the derivative with respect to the clock time for the desired secular change in z over a long time scale. Assuming that the averaged states a, $\tilde{h}$, $\tilde{k}$, and i and control coefficients u_2 and u_3 in Eq. (12) vary slowly [i.e., $d(\,)/dT = \mathcal{O}(\varepsilon)$], then the z state derivative may be written

$$\frac{dz}{dt} = \varepsilon\frac{dz}{dT} = \varepsilon\sqrt{2z}\frac{n\sin i}{8}(\tilde{h}u_2 - \tilde{k}u_3) + \varepsilon^2\frac{n^2\sin^2 i}{64}[(u_2^2 + u_3^2) - 4\tilde{h}\,\tilde{k}\,u_2u_3]t + \mathcal{O}(\varepsilon^3 t) \tag{13}$$

where $T = \varepsilon t$. As expected, this derivative is small ($\mathcal{O}(\varepsilon)$), and so the libration mean-square state is nearly constant over short time intervals. Although the second term on the right-hand side of the derivative in Eq. (13) causes quadratic growth (or decay) of the z state, it is of order ε^2 and may only be significant when considering larger time spans. This derivative will serve as a dynamic constraint in subsequent optimal control problems to manage the magnitude of libration while performing orbital maneuvers. Note that using this model, the change in the libration mean-square state is achieved primarily through the u_2 and u_3 coefficients corresponding to the periodic control resonant with the orbital frequency. This is because in the satellite frame, the local magnetic field vector varies with the orbital frequency. Therefore, resonating control current with this frequency can dampen (or excite) libration.

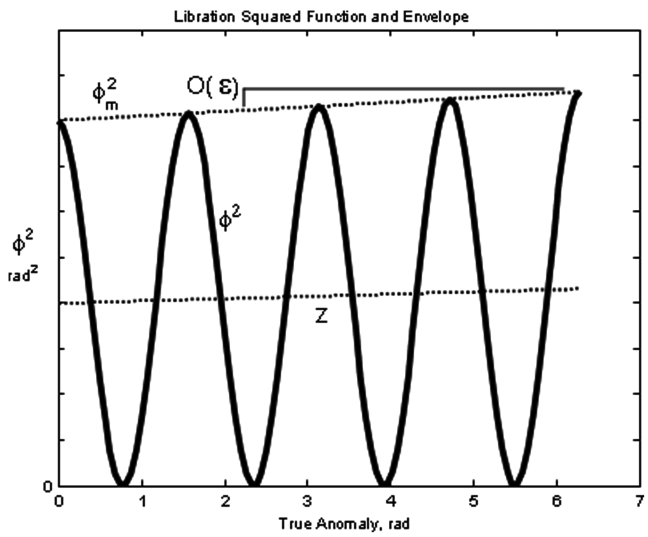

Fig. 4 Libration squared function, mean-square libration function and envelope.

III. Optimal Orbit Transfer Example

With the dynamics of the libration mean-square state in hand, it is possible to optimally maneuver an EDT satellite to a new desired orbit while simultaneously controlling the out-of-plane libration (within the limits of the dynamic model). For this example, we assume that the out-of-plane libration is much larger than the in-plane libration (i.e., $\theta \ll \phi$). Furthermore, the eccentricity and the maximum possible electrodynamic torque for a given tether design are both small (i.e., $e \ll 1$ and $\varepsilon \ll 1$).[¶] Because an EDT must orbit low enough to take advantage of the Earth's magnetic field, the orbit is circular by necessity, and so the problem posed here is for a nearly circular orbit. A 500 kg, 4 km EDT is used in this example with a 230 kg upper end body and a 220 kg lower end body with a maximum rms current of 1.5 A. The optimal controls for this maneuver were determined under three separate sets of conditions for comparison. First, we assumed no drag when performing the maneuver with libration control on. For the second run, we assumed no drag or libration control to compare the results with the first run. Finally, we included drag in the dynamic model and determined the optimal maneuver with active libration damping turned on. These OCPs were solved using DIDO, an optimization software package that discretizes and solves general optimization problems using a pseudospectral method [12,13]. A pseudospectral method was chosen for its relatively high accuracy and short solve times using only a few nodes.

A. Optimal Control Problem Formulation

It is desired to transfer the EDT from a parking orbit at 270 km altitude with an eccentricity of 0.005 and a 30 deg inclination to a 280 km orbit with a 30.5 deg inclination in the minimum-time. While performing this maneuver, the control current must drive the maximum out-of-plane libration angle from 5 down to 3 deg. The OCP is constructed as follows:

$$\begin{aligned}
&\text{Minimize cost: } J = t_f\\
&\text{Subject to: } d\mathbf{x}/dt = \mathbf{f}(\mathbf{x},\mathbf{u})\\
&\mathbf{e_0}[\mathbf{x}(T_0)] = [a_0, e_0, i_0, z_0]^T\\
&\quad = [6648\ \text{km}, 0.005, 30\,\text{deg}, 0.0038\ \text{rad}^2]^T\\
&\mathbf{e_f}[\mathbf{x}(T_f)] = [a_f, i_f, z_f]^T = [6658\ \text{km}, 30.5\,\text{deg}, 0.0014\ \text{rad}^2]^T\\
&g_1[\mathbf{u}(T)] = I_{\text{rms}}^2 - 2.25 \le 0\ \text{A}^2
\end{aligned} \tag{14}$$

where $\mathbf{x}(T) = [a, h, k, i, z]^T$ represents the average states with averaged dynamics $\mathbf{f}(\mathbf{x},\mathbf{u})$ described by Eqs. (2) and (13). Initial and final conditions are given in the form of event equality constraints $\mathbf{e_0}$ and $\mathbf{e_f}$, and the initial eccentricity is given by $e_o = h_o^2 + k_o^2$. The path constraint g_1 bounds the rms current, which is determined by Parseval's theorem in the following form:

$$I_{\text{rms}}^2 = I_m^2[u_1^2 + \tfrac{1}{2}(u_2^2 + u_3^2 + u_4^2 + u_5^2)]$$

Because the rms current is proportional to the average power, this constraint is equivalent to limiting the maximum average power available for thrusting. Finally, states, controls, and time are bounded by upper and lower limits (denoted using subscripts u and l, respectively). These box constraints are written as

$$\mathbf{x}_l \le \mathbf{x}(T) \le \mathbf{x}_u \quad \mathbf{u}_l \le \mathbf{u}(T) \le \mathbf{u}_u \quad T_{0l} \le T_0 \le T_{0u} \quad T_{fl} \le T_f \le T_{fu}$$

[¶]This method of averaging would work with eccentric orbits as well, but one would need to expand about the difference from a reference eccentricity instead of the eccentricity itself.

where we have chosen the bounds to be

$$\mathbf{x}_u = [16,000\ \text{km}, 0.4, 0.4, 80\,\text{deg}, 0.0055\ \text{rad}^2]^T$$
$$\mathbf{x}_l = [6638\ \text{km}, -0.4, -0.4, 15\,\text{deg}, 0\ \text{rad}^2]^T$$
$$\mathbf{u}_u = [1, \sqrt{2}, \sqrt{2}, \sqrt{2}, \sqrt{2}]^T \qquad \mathbf{u}_l = -\mathbf{u}_u \qquad T_0 = 0$$
$$T_f = 50P$$

with initial orbital period P.

B. Results

Before using the optimization solver, the states and time were scaled to span values of order 1 to make the problem numerically well-conditioned ([8,14] each contain a full discussion on scaling for numerical optimization). Solving this problem using DIDO for the no-drag case yields an optimal control solution that drives the libration magnitude to the final desired value while executing the desired orbital maneuver in 222 revolutions. The control solution without drag depicted in Fig. 5 indicates that the optimal strategy is to initially apply a negative dc control current, indicated by u_1, to descend as shown in Fig. 6. Because drag has not yet been introduced to the dynamic model, reducing the orbit size enhances inclination changing capability, as shown by Eq. (2). The controller applies large ac control components cycling at twice the orbital frequency to reach the desired inclination (i.e., large u_4 and u_5 components). The dc component slowly transitions to positive flow by the end of the trajectory, forcing the vehicle to climb to the final desired orbital altitude. There is a small component of the periodic current allotted to u_2 and u_3, which drive the libration amplitude to the desired final

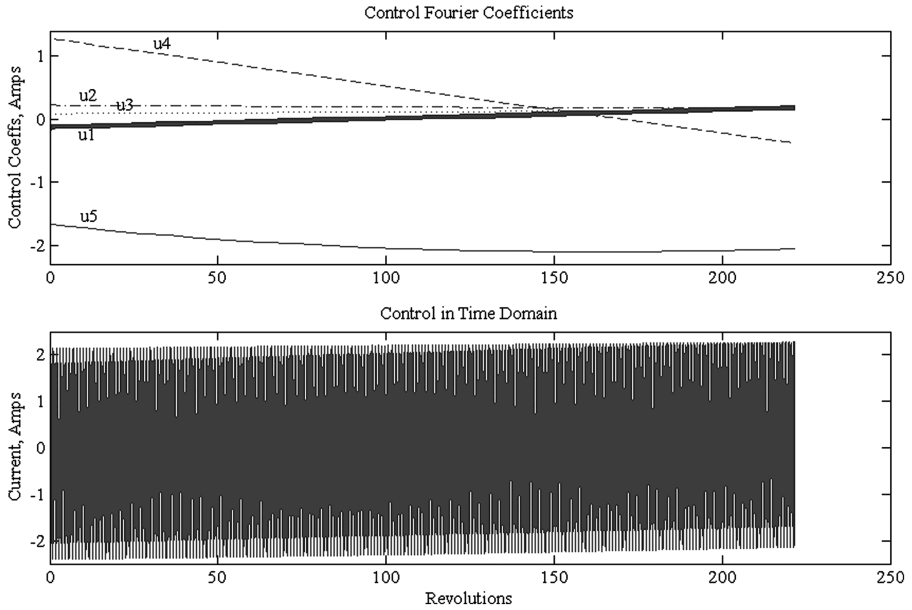

Fig. 5 Control for minimum-time orbit change with libration control, no drag.

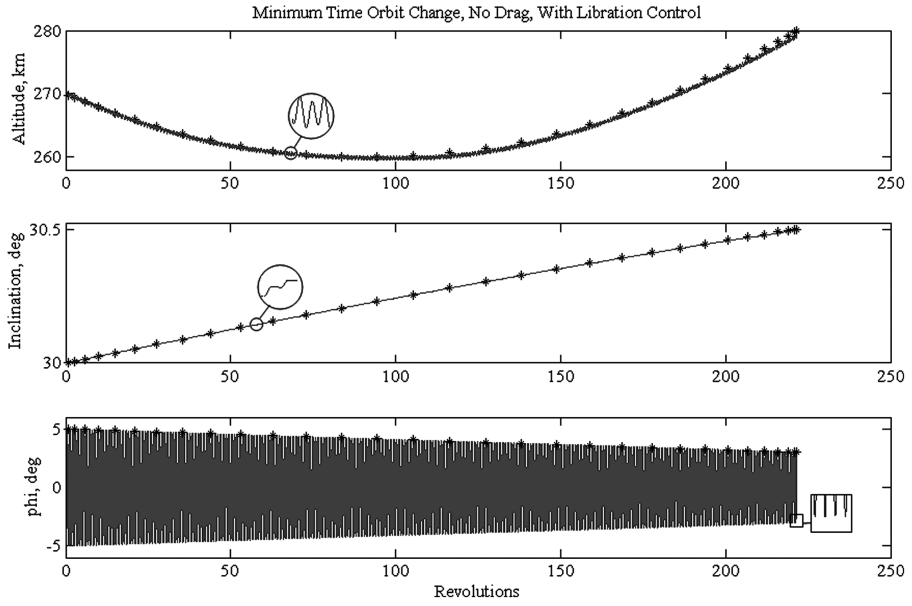

Fig. 6 Minimum-time orbit change state trajectory, no drag. Stars indicate DIDO-derived averaged states; lines indicate propagated instantaneous state.

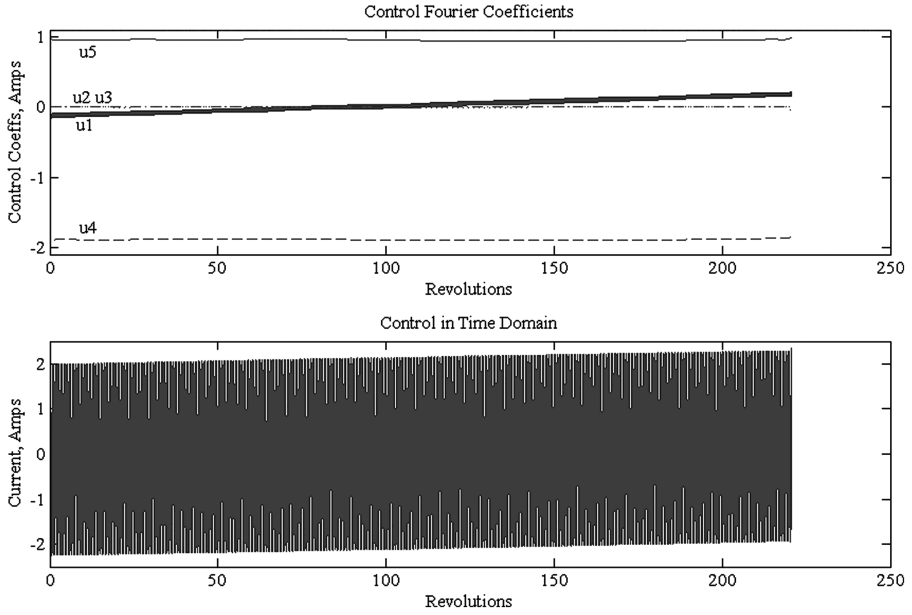

Fig. 7 Control profile for a minimum-time orbit change with no libration control, no drag.

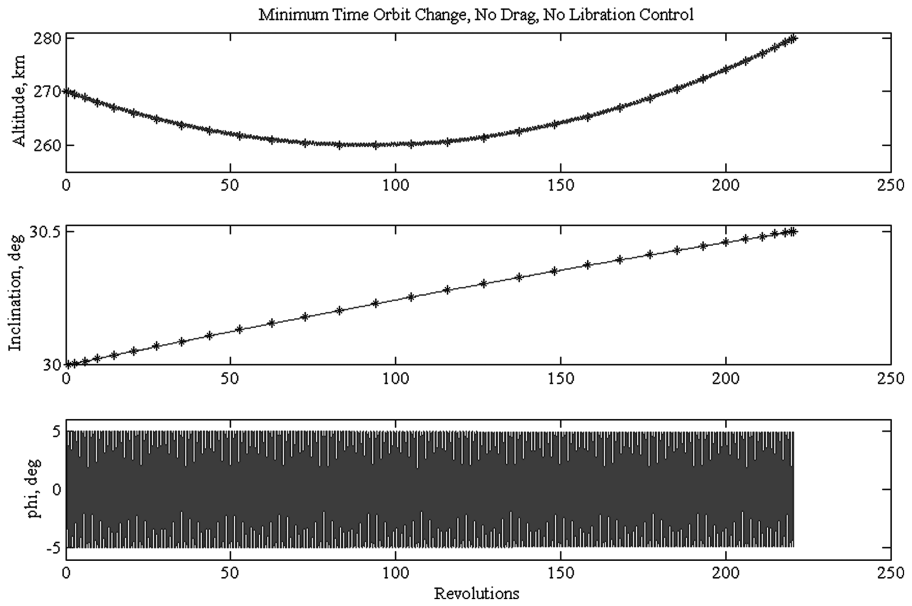

Fig. 8 Minimum-time orbit change state trajectory, no libration control or drag.

state as expected in light of Eq. (13). The orbital states and libration angle depicted in Fig. 6 were propagated using the exact equations of motion given by the general perturbation equations of motion and Eqs. (3) and (4) with a stiff ordinary differential equation solver to verify the accuracy of the dynamic model and the assumptions. DIDO output of the averaged states is depicted by stars and the propagated solution to the exact equations of motion using the DIDO-derived controls is represented by the line. A discussion on the propagation using stiff solvers and numerical round-off errors is provided in [9].

For comparison, a similar constant eccentricity optimal maneuver was executed without any restriction on the libration mean-square state. The constraints in Eq. (14) were enforced with the following exception and addition:

$$\mathbf{e}_{\mathbf{f}}[\mathbf{x}(T_f)] = [a_f, i_f]^T = [6658\ \text{km}, 30.5\,\text{deg}]^T$$

$$g_2[\mathbf{u}(T)] = h^2 + k^2 - e_0^2 = 0$$

Path constraint g_2 ensures that the average eccentricity remains constant throughout the maneuver. The resulting control profile Fig. 7 and trajectory Fig. 8 demonstrate that the maneuver is only marginally quicker (221 revolutions), but the libration amplitude, left uncontrolled, remains practically unchanged for this time span. Given enough time, however, this amplitude can grow in a thrusting tether, and so it is important to manage the libration while maneuvering an EDT. This is especially true for a tether that is long, carries a large control current, or has a large mass differential between the upper and lower masses, resulting in a large electrodynamic torque when the EDT is active. The maneuver is executed while avoiding large components of periodic current cycling at the orbital frequency (i.e., u_2 and u_3), which are large contributors to eccentricity change.

When drag is included in the dynamic model [i.e., $D \neq 0$ in Eq. (2)], the control profile is completely different from the no-drag case. A climb-and-descend strategy is employed in which the controls initially boost the satellite to take advantage of the lower atmospheric density at higher altitudes, where power may be

dedicated to increasing the orbit inclination without having to compete with a large dc component that would be required to compensate for drag. The controls are shown in Fig. 9, with the resulting trajectory shown in Fig. 10, which includes the in-plane libration history propagated using Eq. (3). With drag, this maneuver takes three more days to complete than its no-drag counterpart, requiring a total of 270 revolutions. Solving this large-time-scale problem in the time domain would be a daunting task even for the best available optimization programs, which would require an absolute minimum of 4 nodes per revolution to capture the periodic nature of this problem. The averaged state solution, on the other hand, requires only a few nodes and is reminiscent of a Zermelo-type solution, which provides the minimum-time path between two points in a vector field.

C. Optimality

Although we do not demonstrate definitive optimality of the control solution, we will show compliance with one transversality condition necessary for optimality. Because there is no explicit time dependence in the Lagrangian of the Hamiltonian of this optimal control problem, we have $\dot{\bar{H}} = 0$. The Lagrangian of the Hamiltonian is defined as

$$\bar{H} = H + \mu_g g_1 + \boldsymbol{\mu}_x^T \mathbf{x} + \boldsymbol{\mu}_u^T \mathbf{u}$$

where the Hamiltonian for this Mayer cost optimal control problem is defined by $H = \boldsymbol{\lambda}^T \mathbf{f}$, and $\boldsymbol{\lambda}$ represents the costate vector. The covector functions associated with the path constraint, state-variable box constraints and control-variable constraints are represented by μ_g, $\boldsymbol{\mu}_x$, and $\boldsymbol{\mu}_u$, respectively. Furthermore, because the problem posed here is a minimum-final-time problem, we have $\bar{H}(t_f) = -1$, and so we have a condition that holds throughout the trajectory: namely,

$$\bar{H}(t) = -1 \tag{15}$$

DIDO uses the covector mapping principle [15] to produce adjoints

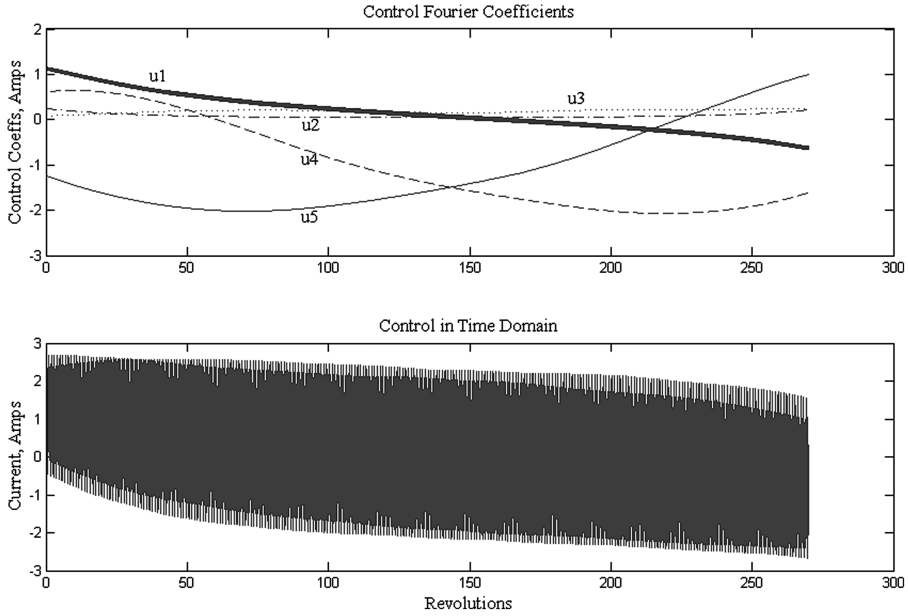

Fig. 9 Control profile for a minimum-time orbit change with libration control and drag.

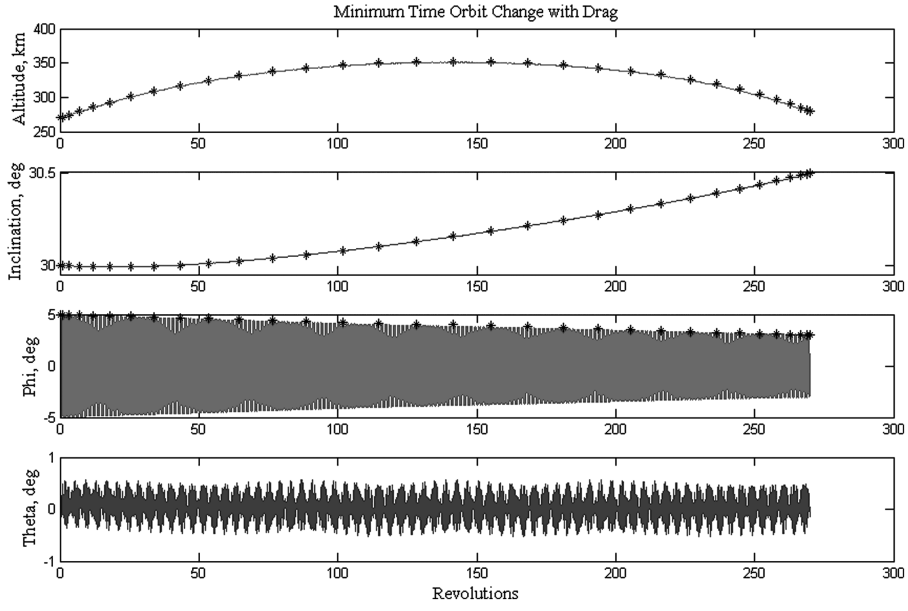

Fig. 10 Minimum-time orbit change state trajectory with drag.

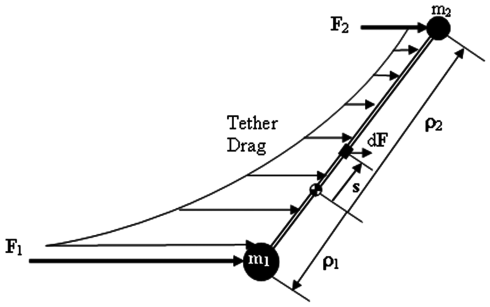

Fig. 11 Tether subject to atmospheric drag.

and the Hamiltonian as part of the solution, and we were able to verify that the DIDO-derived Hamiltonian indeed satisfied the optimality condition given in Eq. (15) throughout the trajectory within a tolerance of 0.002. Several other solutions were generated using a different number of collocation node points and slightly different endpoint constraints, and the results were similar to those presented here.

IV. Conclusions

Solving some periodic optimal control problems in Fourier space using large time scales and time-averaged states has significant advantages when the desire is to control the secular behavior of a state over a long time, rather than the instantaneous behavior. Using this method, complex optimal control problems normally requiring thousands of optimization nodes may be transformed into simple problems in Fourier space, requiring only a few dozen nodes. For a continuously operating low-thrust satellite, a rapidly changing periodic variable may be averaged out of the dynamics, leaving only the dynamics of the slowly changing averaged variables. In the case of electrodynamic tethers, including a state that captures the magnitude of the out-of-plane tether libration provides a higher-fidelity constraint model that enables more accurate optimal control and also provides a mechanism to achieve stability. Because the averaged equations of motion for orbit transfers assume a near nadir-pointing tether, bounding the libration to small values is even more critical. The results demonstrate that it is possible to control tether libration while simultaneously maneuvering to a new orbit using periodic control of the EDT current over a long time scale. This method of controller design could assist engineers with design trade studies offering not only feasible solutions, but quick and accurate nearly optimal solutions. Implemented as a far horizon controller, this method could be used to determine a long-term control strategy, then uplink control coefficients to a satellite that would then feed these commands to an instantaneous state controller.

Appendix: Derivation of Libration Equations of Motion

In developing an orbital maneuvering controller, it is important to understand the libration behavior of tether motion that is subject to electrodynamic and aerodynamic forces. A thorough derivation of the libration equations of motion is presented in [2,9], but key results are presented here for convenience. The tether is modeled as two end masses connected by a straight tether in constant tension with a uniform mass distribution (rigid-dumbbell model). The conservative gravitational force plays a large role in the tether libration dynamics and lends itself well to the development of equations of motion using the Lagrangian method. The following derivation follows the Lagrangian method using coordinates in the rotating frame shown in Fig. 3. The inertial frame is centered at the center of the Earth. The rotating frame is located at a position $\mathbf{r}$ with respect to the inertial frame and is centered at the system center of mass (COM). It consists of three mutually orthogonal unit vectors: $\hat{\mathbf{e}}_\mathbf{r}$ in the zenith direction, $\hat{\mathbf{e}}_\mathbf{t}$ in the transverse direction, and $\hat{\mathbf{e}}_\mathbf{n}$ completing the triad in the direction perpendicular to the orbital plane. The vectors along the straight tether extending from the COM to mass 1 and mass 2 are $\boldsymbol{\rho}_1$ and $\boldsymbol{\rho}_2$, respectively.

Under the assumptions of the dumbbell model, the total kinetic energy may be decomposed into two parts. One contribution is due to the bulk translational motion of the system acting at the center of mass, and another contribution is due to the motion about the COM. The kinetic energy is therefore written as

$$T = \tfrac{1}{2}m\dot{\mathbf{r}}\cdot\dot{\mathbf{r}} + \tfrac{1}{2}\tilde{m}(\dot{L}^2 + L^2\boldsymbol{\Omega}\cdot\bar{\bar{\mathbf{J}}}\cdot\boldsymbol{\Omega}) \tag{A1}$$

where L is the tether length and $\tilde{m}$ is the equivalent reduced mass, which accounts for the mass distribution of the entire system and is written [3,9]

$$\tilde{m} = \frac{1}{m}\left(m_1 + \frac{m_t}{2}\right)\left(m_2 + \frac{m_t}{2}\right) - \frac{m_t}{6}$$

The total system mass m is composed of the lower end-body mass m_1, the upper end-body mass m_2, and the tether mass m_t. Dots here indicate differentiation with respect to time [i.e., $(\dot{}) = d()/dt$]. Assuming that the tether does not stretch or go slack (i.e., $\dot{L} = 0$), then the second term on the right-hand side of Eq. (A1) represents kinetic energy due to the rotational motion about the COM, where $\tilde{m}L^2\bar{\bar{\mathbf{J}}}$ is the moment of inertia tensor ($\bar{\bar{\mathbf{J}}} \approx \text{diag}[0, 1, 1]$) and $\boldsymbol{\Omega}$ is the angular velocity of the tether expressed using tether body coordinates. Given the tether angular velocity $\boldsymbol{\omega}_\mathbf{e} = [\dot{\theta}\sin\phi, -\dot{\phi}, \dot{\theta}\cos\phi]^T$, we write

$$\boldsymbol{\Omega} = \dot{\boldsymbol{\nu}} + \boldsymbol{\omega}_\mathbf{e} = [\,(\dot{\theta}+\dot{\nu})\sin\phi \quad -\dot{\phi} \quad (\dot{\theta}+\dot{\nu})\cos\phi\,]^T$$

Therefore,

$$\boldsymbol{\Omega}\cdot\bar{\bar{\mathbf{J}}}\cdot\boldsymbol{\Omega} = \boldsymbol{\Omega}^T\mathbf{J}\boldsymbol{\Omega} = \dot{\phi}^2 + c^2\phi(\dot{\theta}+\dot{\nu})^2$$

Similarly, the potential energy may be expressed in two parts. One contribution is due to the total system mass acting as a point mass in a potential field, and a second contribution is the gravity gradient potential due to the center of gravity offset from the COM. The potential energy is approximated as

$$V \approx -\frac{\mu m}{r} - \frac{\mu L^2}{2r^3}\tilde{m}[3(\hat{\boldsymbol{\rho}}\cdot\hat{\mathbf{e}}_\mathbf{r})^2 - 1] \tag{A2}$$

where the tether orientation vector expressed in the rotating frame is $\hat{\boldsymbol{\rho}} = [\cos\phi\cos\theta \quad \cos\phi\sin\theta \quad \sin\phi]^T$.

For the rigid-dumbbell model presented here, the Lagrangian is then

$$L = T - V = \frac{1}{2}mv^2 + \frac{1}{2}\tilde{m}L^2[\dot{\phi}^2 + \cos^2\phi(\dot{\theta}+\dot{\nu})^2] + \frac{\mu m}{r} + \frac{\mu\tilde{m}L^2}{2r^3}(3\cos^2\phi\cos^2\theta - 1)$$

The Lagrangian equations of motion for in- and out-of-plane librations are, respectively,

$$\frac{d}{dt}\left(\frac{\partial L}{\partial\dot{\theta}}\right) - \frac{\partial L}{\partial\theta} = Q_\theta$$

$$\tilde{m}L^2\left[\cos^2\phi(\ddot{\theta}+\ddot{\nu}) + 2\dot{\phi}\cos\phi\sin\phi(\dot{\theta}+\dot{\nu}) + \frac{3\mu}{r^3}\cos^2\phi\cos\theta\sin\theta\right] = Q_\theta \tag{A3}$$

and

$$\frac{dL}{dt}\left(\frac{\partial L}{\partial\dot{\phi}}\right) - \frac{\partial L}{\partial\phi} = Q_\phi$$

$$\tilde{m}L^2\left\{\ddot{\phi} + \cos\phi\sin\phi\left[(\dot{\theta}+\dot{\nu})^2 + \frac{3\mu}{r^3}\cos^2\theta\right]\right\} = Q_\phi \tag{A4}$$

where Q_θ and Q_ϕ are generalized forces affecting the in- and out-of-plane librations, respectively, due to the electrodynamic Lorenz and

aerodynamic drag forces. These generalized forces are derived as follows.

Because the atmosphere is too thin at relevant orbital altitudes to model as a fluid, we use a free-molecular flow model instead [16]; that is, the molecular mean free path is large compared with the dimensions of the satellite. This force acts on both end masses and the tether itself. In general, each end body has a different ballistic coefficient and the system COM is not located at the center of the tether. Furthermore, the atmospheric density varies exponentially along the length of the tether; thus, the impact force of incoming atmospheric particles varies along the wire, as shown in Fig. 11. The generalized in-plane aerodynamic torque depends on the drag on the lower body, $\mathbf{F_1}$, the drag on the upper body, $\mathbf{F_2}$, and the torque about the COM due to the distributed drag along the tether, $\mathbf{M_t}$, and is given by

$$Q_{\theta a} = \mathbf{F_1} \cdot \frac{\partial \mathbf{v_1}}{\partial \dot{\theta}} + \mathbf{F}_2 \cdot \frac{\partial \mathbf{v_2}}{\partial \dot{\theta}} + \mathbf{M_t} \cdot \frac{\partial \mathbf{\Omega}}{\partial \dot{\theta}}$$

The torques due only to the end bodies are given by

$$\mathbf{F_1} \cdot \frac{\partial \mathbf{v}_1}{\partial \dot{\theta}} = \mathbf{F_1} \cdot \frac{\partial \Omega}{\partial \dot{\theta}} \times \boldsymbol{\rho_1}$$
$$= \frac{1}{2} B_1^* \rho(h) e^{p_1} v^2 \mu_m L \cos\phi(\cos\gamma\cos\theta - \sin\gamma\sin\theta)$$
$$\mathbf{F}_2 \cdot \frac{\partial \mathbf{v_2}}{\partial \dot{\theta}} = \mathbf{F_2} \cdot \frac{\partial \Omega}{\partial \dot{\theta}} \times \boldsymbol{\rho_2}$$
$$= -\frac{1}{2} B_2^* \rho(h) e^{-p_2} v^2 \mu_m L \cos\phi(-\sin\gamma\sin\theta + \cos\gamma\cos\theta)$$

where

$$\mu_m = \frac{1}{m}\left(m_1 + \frac{m_t}{2}\right)\left(m_2 + \frac{m_t}{2}\right)$$

is a two-end-body reduced mass and where

$$p_1 = \frac{1}{mh^*}\left(m_2 + \frac{m_t}{2}\right) L\cos\phi\cos\theta$$

and

$$p_2 = \frac{1}{mh^*}\left(m_1 + \frac{m_t}{2}\right) L\cos\phi\cos\theta$$

are factors that capture the adjusted drag at the lower and upper end-body altitudes, respectively, with respect to the drag at a reference altitude h, given an atmospheric scale height h^*. The flight-path angle of the satellite in orbit is represented by γ, and the ballistic coefficients for the lower and upper end bodies are given by B_1^* and B_2^*, respectively, defined by Eq. (1) using respective end-body parameters. The torque due to the distributed nonuniform drag load over the length of the tether is given by

$$\mathbf{M_t} \cdot \frac{\partial \mathbf{\Omega}}{\partial \dot{\theta}} = \oiint \mathbf{s} \times d\mathbf{F} \cdot \frac{\partial \mathbf{\Omega}}{\partial \dot{\theta}} = \rho(h) v^2 E[e^{-p_2}(-p_2 - 1)$$
$$- e^{p_1}(p_1 - 1)]\cos\phi(\sin\gamma\sin\theta - \cos\gamma\cos\theta)$$

where

$$d\mathbf{F} = \frac{C_{dt}}{2}\rho(h) v_a^2 dA \hat{\mathbf{v}}_\mathbf{a}$$

$$E = d_t[1 - \cos^2\phi\sin^2(\theta + \gamma)]^{1/2}\left(\frac{h^*}{\cos\phi\cos\theta}\right)^2$$

and d_t represents the tether diameter. It is assumed that the airflow velocity $\hat{\mathbf{v}}_\mathbf{a}$ is nearly constant along the tether so that drag differential is due only to the difference in atmospheric density. The coefficient of drag for the tether wire, C_{dt}, is approximately 2.

Similarly, aerodynamic torque affecting the out-of-plane libration is

$$Q_{\phi a} = \mathbf{F_1} \cdot \frac{\partial \mathbf{v_1}}{\partial \dot{\phi}} + \mathbf{F}_2 \cdot \frac{\partial \mathbf{v_2}}{\partial \dot{\phi}} + \mathbf{M_t} \cdot \frac{\partial \mathbf{\Omega}}{\partial \dot{\phi}}$$

where

$$\mathbf{F_1} \cdot \frac{\partial \mathbf{v_1}}{\partial \dot{\phi}} = -\frac{1}{2} B_1^* \rho(h) e^{p_1} v^2 \mu_m L \sin\phi(\sin\gamma\cos\theta + \cos\gamma\sin\theta)$$
$$\mathbf{F}_2 \cdot \frac{\partial \mathbf{v_2}}{\partial \dot{\phi}} = \frac{1}{2} B_2^* \rho(h) e^{-p_2} v^2 \mu_m L \sin\phi(\sin\gamma\cos\theta + \cos\gamma\sin\theta)$$
$$\mathbf{M_t} \cdot \frac{\partial \mathbf{\Omega}}{\partial \dot{\phi}} = \rho(h) v^2 E[e^{-p_2}(-p_2 - 1)$$
$$- e^{p_1}(p_1 - 1)]\sin\phi(\sin\gamma\cos\theta + \cos\gamma\sin\theta)$$

The electrodynamic force $\mathbf{F}$ due to a current I traveling through a straight wire with length vector $\mathbf{L}$ in a magnetic field $\mathbf{B}$ is given by

$$\mathbf{F} = I\mathbf{L} \times \mathbf{B} = IL\hat{\boldsymbol{\rho}} \times \mathbf{B}$$

expressed in the rotating frame as

$$\mathbf{F} = IL\begin{bmatrix} B_n\cos\phi\sin\theta - B_t\sin\phi \\ B_r\sin\phi - B_n\cos\phi\cos\theta \\ B_t\cos\phi\cos\theta - B_r\cos\phi\sin\theta \end{bmatrix}$$

The Lorenz torque affecting the in-plane libration is

$$Q_{\theta e} = \mathbf{F} \cdot \frac{\partial \mathbf{v}}{\partial \dot{\theta}} = \mathbf{F} \cdot \left(\frac{\partial \mathbf{\Omega}}{\partial \dot{\theta}} \times \boldsymbol{\rho_t}\right)$$

where

$$\boldsymbol{\rho}_\mathbf{t} = \frac{(m_2 - m_1)L}{2M}\hat{\boldsymbol{\rho}}$$

represents the moment arm of the resultant Lorenz force at the center of the tether with respect to the COM.

In the rotating frame, this torque is

$$Q_{\theta e} = IL\rho_t(\cos\phi\cos\theta\sin\phi B_r + \sin\phi\cos\phi\sin\theta B_t - \cos^2\phi B_n)$$

Similarly, the Lorenz torque affecting the out-of-plane libration is

$$Q_{\phi e} = \mathbf{F} \cdot \frac{\partial \mathbf{v}}{\partial \dot{\phi}} = \mathbf{F} \cdot \left(\frac{\partial \mathbf{\Omega}}{\partial \dot{\phi}} \times \boldsymbol{\rho_t}\right)$$

expressed in the rotating frame as

$$Q_{\phi e} = IL\rho_t(-\sin\theta B_r + \cos\theta B_t)$$

The total generalized forces (torques) are the sum of the torques due to the electrodynamic and aerodynamic forces:

$$Q_\theta = Q_{\theta a} + Q_{\theta e} \qquad Q_\phi = Q_{\phi a} + Q_{\phi e}$$

These terms may be substituted into Eqs. (A3) and (A4) to fully describe the instantaneous librational motion of the EDT system.

References

[1] Lorenzini, E., and Sanmartin, J., "Electrodynamic Tethers in Space," *Scientific American*, Vol. 291, No. 2, Aug. 2004, pp. 50–57.

[2] Pelaez, J., Lorenzini, E. C., Lopez-Rebollal, O., and Ruiz, M., "A New Kind of Dynamic Instability in Electrodynamic Tethers," *Journal of the Astronautical Sciences*, Vol. 48, No. 4, 2000, pp. 449–476.

[3] Williams, P., "Optimal Orbital Transfer with Electrodynamic Tether," *Journal of Guidance, Control, and Dynamics*, Vol. 28, No. 2, 2005, pp. 369–371. doi:10.2514/1.12016

[4] Carroll, J., "Guidebook for Analysis of Tether Applications," Martin Marietta Corp., CR RH4-394049, Mar. 1985, p. 31.

[5] Tragesser, S. G., and San, H., "Orbital Maneuvering with Electrodynamic Tethers," *Journal of Guidance, Control, and Dynamics*, Vol. 26, No. 5, 2003, pp. 805–810. doi:10.2514/2.5115

[6] Stevens, R. E., and Wiesel, W., "Large Time Scale Optimal Control of an Electrodynamic Tether Satellite," *Journal of Guidance, Control, and Dynamics*, Vol. 31, No. 6, 2008, pp. 1716–1727. doi:10.2514/1.34897

[7] van Heijenoort, J., *Frege to Godel: A Source Book in Mathematical Logic, 1879–1931*, Harvard Univ. Press, Cambridge, MA, 1967.

[8] Ross, I. M., Gong, Q., and Sekhavat, P., "Low-Thrust, High-Accuracy Trajectory Optimization," *Journal of Guidance, Control, and Dynamics*, Vol. 30, No. 4, 2007, pp. 921–932. doi:10.2514/1.23181

[9] Stevens, R. E., "Optimal Control of Electrodynamic Tether Satellites," Ph.D. Dissertation, Department of Aeronautics and Astronautics, Air Force Institute of Technology, Wright–Patterson AFB, OH, 2008.

[10] Fowles, G. R., and Cassiday, G. L., *Analytical Mechanics*, 6th ed., Saunders College Publishing, Orlando, Florida, 1999, pp. 442–443.

[11] Pelaez, J., and Lorenzini, E. C., "Libration Control of Electrodynamic Tethers in Inclined Orbit," *Journal of Guidance, Control, and Dynamics*, Vol. 28, No. 2, Mar.–Apr. 2005, pp. 269–279. doi:10.2514/1.6473

[12] Ross, I. M., and Fahroo, F., *Legendre Pseudospectral Approximations of Optimal Control Problems*, Lecture Notes in Control and Information Sciences, Vol. 295, Springer–Verlag, New York, 2003, pp. 327–342.

[13] DIDO, Software Package, Ver. 7.3.2, Elissar, LLC, Monterey, CA, 2007.

[14] Ross, I. M., "A Beginner's Guide to DIDO (Ver. 7.3)," TR-710, Elissar, LLC, Monterey, CA, 2007.

[15] Gong, Q., Ross, I. M., Kang, W., and Fahroo, F., "On the Pseudospectral Covector Mapping Theorem for Nonlinear Optimal Control," *45th IEEE Conference on Decision and Control*, Inst. of Electrical and Electronics Engineers, Piscataway, NJ, Dec. 2006, pp. 2679–2686.

[16] Beletsky, V., and Levin, E., *Dynamics of Space Tether Systems*, Advances in the Astronautical Sciences, Vol. 83, American Astronautical Society, San Diego, CA, 1993, pp. 200–205.